

INTERACTIONS OF XANTHONE COMPOUNDS FROM THE MANGOSTEEN (*GARCINIA MANGOSTANA* L) PERICARPS AGAINST INOS, COX-1, AND COX-2 ENZYME RECEPTORS AS ANTI-INFLAMMATORY

DWINTHA LESTARI^{1*} , RISKA PERMATA SARI¹ , IDA MUSFIROH² , SANDRA MEGANTARA² , MEILINDA SETYA PRACEKA³ , NUR KUSAIRA KHAIRUL IKRAM⁴ , MUCHTARIDI² 

¹Department of Pharmacy, Universitas Muhammadiyah Bandung, Indonesia, ²Department of Pharmaceutical Analysis Pharmacy and Medicinal Chemistry, Faculty of Pharmacy, Universitas Padjadjaran, Indonesia, ³Department of Pharmacy, Universitas Halim Sanusi, Bandung, Indonesia, ⁴Institute of Biological Sciences, Faculty of Science, University of Malaya, Kuala Lumpur, Malaysia
*Email: dwintha85@gmail.com

Received: 18 Jul 2022, Revised and Accepted: 17 Oct 2022

ABSTRACT

Objective: Mangosteen is a plant that is very effective for inflammation. Besides that, the skin of the mangosteen plant in Indonesia continues to be developed because it is an antioxidant and suppresses the production of cytokines.

Methods: Screening pharmacophores and molecular docking simulations by molecular modeling computation to predict the activity of the Mangosteen plant *in silico* and to determine potential drug candidates from mangosteen for inflammation to the iNOS, COX-1, and COX-2.

Results: Pharmacophore Screening, γ -mangosteen has the highest pharmacophore fit score of 33.32 and 33.64 on COX-1 and COX-2 and is selective to iNOS target. Molecular docking of α -mangosteen and γ -mangosteen test compounds to the active site of used, COX-1, and COX-2 enzymes showed free energy binding (ΔG°) values of, -5.09, -5.00, -6.15; and -6.76, -5.30, -7.81 Kcal/mol respectively. Meanwhile, hydrogen bonds and good ΔG° values were formed between γ -mangosteen and COX-2, where the Hydroxyl group on γ -mangosteen interacted with the amino acids His75, Ser339, and Ala513 with ΔG° of -7.81 Kcal/mol.

Conclusion: It can be said that α -mangosteen and γ -mangosteen have molecular interactions with COX-1 and COX-2 active sites with the highest affinity for COX-2 compared to COX-1, and iNOS.

Keywords: Anti-inflammatory, iNOS, COX-1, and COX-2, Pharmacophore, Ligandscout, Molecular docking, α -mangosteen, and γ -mangosteen

© 2023 The Authors. Published by Innovare Academic Sciences Pvt Ltd. This is an open-access article under the CC BY license (<https://creativecommons.org/licenses/by/4.0/>)
DOI: <https://dx.doi.org/10.22159/ijap.2023v15i1.45861>. Journal homepage: <https://innovareacademics.in/journals/index.php/ijap>

INTRODUCTION

The use of plants as medicine is considered to be safer than synthetic drugs. One of the traditional medicinal plants with anti-inflammatory potential is mangosteen (*Garcinia mangostana* L.), especially its rind. Several studies have shown that the rind of the mangosteen fruit contains compounds that have pharmacological and antioxidant activities. These compounds include flavonoids, tannins, and xanthenes [1, 2].

The mangosteen fruit is rich in nutrients called xanthenes which are abundant in the skin of the fruit [3]. Several studies have shown that the largest component of the mangosteen fruit is the skin, which is 70-75%, while the flesh is only 10-15% and the seeds are 15-20%. The highest xanthone content is found in the mangosteen rind, which is 107.76 mg per 100 g of rind [4]. However, several xanthone derivatives have beneficial pharmacological activities such as anti-inflammatory, antihistamine, antibacterial, and antifungal and have been used for the treatment or therapy of heart disease and HIV. One of the xanthone derivatives is mangosteen [2, 5].

Mangosteen and its derivatives belong to the xanthone groups that are yellow phenolic pigments whose color reactions and chromatographic movements are similar to those of flavonoids. The main content in xanthenes is the content of alpha-mangosteen and gamma-mangosteen. Alpha-mangosteen is a compound that is very efficacious in suppressing the formation of carcinogenic compounds in the colon. In addition to alpha-mangosteen, xanthone compounds also contain gamma-mangosteen, which is beneficial for the protection and prevention of diseases, such as inflammation [5].

Inflammation is the body's defense response against foreign body invasion, tissue damage, or both, caused by microorganisms, mechanical trauma, chemical substances, and physical influences. Symptoms of the anti-inflammatory response can be reborn (redness), heat, dolor (pain), and tumor (swelling). Prostaglandins

(PG), arachidonic acid (AA) metabolites of cyclooxygenase (COX), are the major mediators in the regulation of inflammation and immune function [1]. PGs (prostaglandins) are mediators of inflammation that can be formed from arachidonic acid by consumptive enzymes, namely COX-1 and COX-2 [6].

Previous studies reported that α -mangosteen can significantly inhibit nitric oxide (NO), prostaglandin E2 (PGE2), tumor necrosis factor (TNF)- α , and iNOS (iNOs) induced production in lipopolysaccharide-stimulated RAW 264.7 cells (LPS) [7]. In addition, γ -mangosteen has an inhibitory effect on receptors ranging from the peripheral nervous system and central nervous system as well as lipopolysaccharide that stimulates the stimulation of (sodium oxide) production, which has anti-inflammatory effects and cyclooxygenase-2 (COX-2) and prostaglandin E2 (PGE2) [8].

This study determines the pharmacophore fit score, affinity, and interaction of α -mangosteen and γ -mangosteen compounds, COX-1, and COX-2 enzymes by determining the hydrogen bonds and the selectivity of mangosteen compounds to iNOS enzymes, COX-1, and COX-2 using the molecular docking method.

MATERIALS AND METHODS

Materials

Hardware: Laptop Intel @ CPU 2 Core N3350 processor up to 2.4 GHz and 2 GB RAM.

Software: ChemDraw 8.0, Discovery Studio, GaussView 8.0, Ligandscout 4.4.5 [9], Autodock Tools 1.5.6., Protein Data Bank (PDB) (<http://www.rcsb.org>) [10], Pub Chem (<http://pubchem.ncbi.nlm.nih.gov/>) [11], and database active-decoys used dude (<http://dude.docking.org/>) [9, 12] were used in this study [13]. The ligand structure was drawn using Chemdraw software and the structure was optimized using the Gaussian

software. In addition, protein structures were downloaded from the PDB (Protein Data Bank), including iNOS (PDB code: 1NSI), COX-1 (PDB code: 1EQG), and COX-2 (PDB code: 3LN1).

Methods

Pharmacophore modeling

Preparation of active, decoys, and testing databases using LigandScout 4.4. In structural modeling, a total of 10 models were validated using the enrichment factor parameter (EF 1%) to determine the specificity, accuracy, sensitivity values, and Receiver Operating Characteristics (ROC) of the Area Under Curve (AUC 100%). Pharmacophore screening was carried out based on a selected best model against a database of test compounds consisting of γ -mangosteen, α -mangosteen, ibuprofen, celecoxib, and L-arginine [9].

Enzyme preparation of iNOS, COX-1, and COX-2

The protein targets were downloaded from the protein data bank (PDB). The enzyme receptor preparation stage was carried out by separating the native ligand portion of the enzyme receptor using the Discovery Studio [14].

Docking validation method

The Molecular docking validation was carried out by redocking between the native ligands and the target protein with Autodock 4.4. This validation was valid with the parameter value of RMSD less than 3 Å (Root Mean Square Distance) [15]. For the validation of the moorings carried out on the natural ligand iNOS enzyme, L-arginine was used. COX-1 binding validation was carried out with its natural ligand, ibuprofen, and for the validation of the binding of the COX-2 enzyme, the crystalline, which was Celecoxib. Was isolated, and validation was carried out for binding site analysis to see an interaction between each natural ligand against the enzyme receptor and to determine the amino acid residues of the iNOS, COX-1, and COX-2 enzyme binding pockets [16].

Optimization of the 3d structure of α -mangosteen and γ -mangosteen

The test compound with a 3D shape was optimized using the GaussView 8.0 program using the AM1 semi-empirical method. Each analog is taken in the conformation with the lowest energy and stored in (.mol2 format) or in (.pdb format) as the ligand to be docked.

Molecular docking of α -mangosteen and γ -mangosteen on iNOS, COX-1, and COX-2 enzymes

The optimized test compound was then attached to the iNOS, COX-1, and COX-2 enzyme receptors without their natural ligands using Autodock Tools 1.5.6 software. This tethering process uses a grid box and the parameters of the valid tethering validation method [14].

Data analysis

The resulting energy results in the form of bond-free energy (ΔG°), which shows the bond of the test compound with the target protein. The more negative the energy of a bond produced, it indicates that the stronger and more stable the bond between the test compound and the target protein is. The interaction can be seen from the type of bond formed and the visualization of the binding of molecules between α -mangosteen and γ -mangosteen with iNOS, COX-1, and COX-2 enzymes.

RESULTS AND DISCUSSION

Screening pharmacophore of iNOS, COX-1, and COX-2

For each database, active and decoys on COX-1, COX-2, and iNOS targets used a ratio (100:400). Pharmacophore modeling was done by creating 10 structure models that automatically derive their chemical features. During the pharmacophore screening, each ligand was analyzed for its geometrical structural similarity based on the 3D pharmacophore features [17]. Method validation was done by selecting the best model with specificity>0.5, sensitivity>0.5, hit score>0.7 and AUC>0.7 [18]. The following method validation results (fig. 1) Represent the best model of the ROC curve of the COX-1, COX-2, and iNOS targets [9].

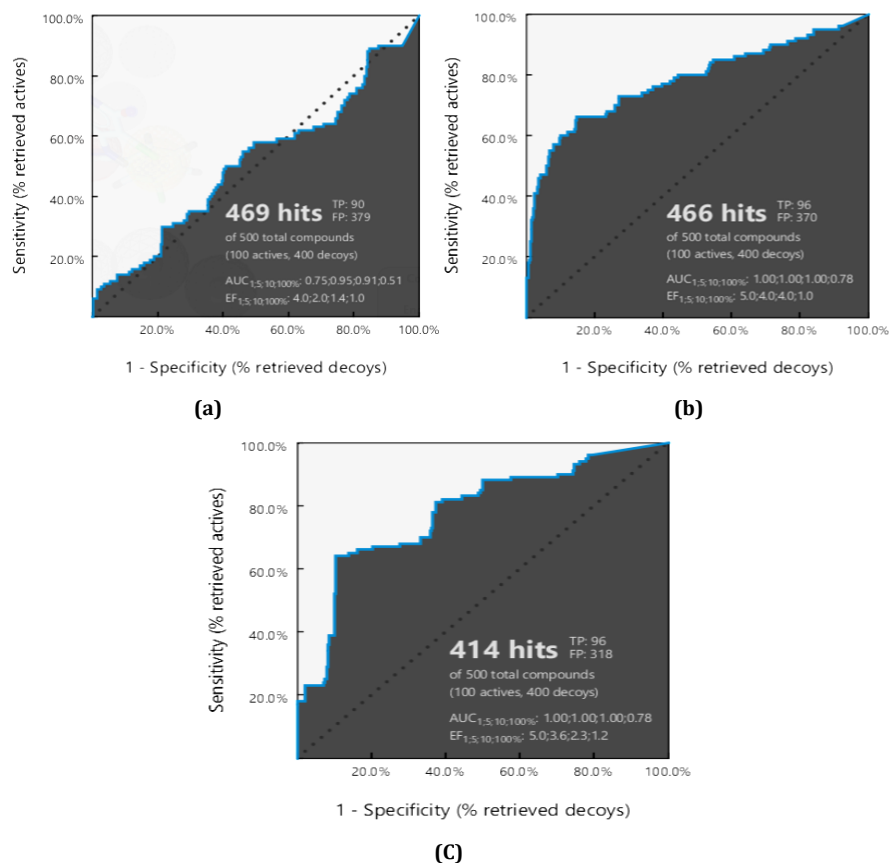


Fig. 1: ROC of (a) COX-1, (b) COX-2, and (c) iNOS

Based on the results, the value of Area Under Curve ($AUC_{100\%}$) and enrichment factor ($EF_{100\%}$) iNOS; COX-1 (0.75 and 4.0), COX-2 (1.00 and 5.0), and iNOS (1.00 and 5.0). These quality parameters are the most common parameters for evaluating pharmacophore modeling through the ROC curve. AUC and EF values can indicate an excellent screening method used for screening virtual pharmacophores [18].

The best-validated model was then used in virtual pharmacophore screening to test the suitability of the pharmacophore 3D structure via the percentage yield value of the geometrical structure similarity compared with the chemical features of the pharmacophore 3D model [19]. On table 1 are the results of virtual pharmacophore screening.

Table 1: Screening pharmacophore

Target name	Compound with hits	Pharmacophore features	Pharmacophore fit	The best model	ROC
COX-1	γ -mangosteen		33.32	Model 8	AUC= 0.75 EF= 4.0
	α -mangosteen		32.50		
	Ibuprofen		32.30		
COX-2	γ -mangostin		33.64	Model 9	AUC= 1.00 EF= 5.0
	α -mangostin		31.14		
	Ibuprofen		33.09		
	Celecoxib		31.90		
iNOS	-	-	-	Model 2	AUC= 1.00 EF= 5.0

Based on the results of screening, γ -mangosteen had the highest chemical features and pharmacophore values, with 33.32 and 33.64 on COX-1 and COX-2 targets compared to α -mangosteen, ibuprofen, and celecoxib. This indicates that γ -mangosteen has a better affinity and is more selective for COX-1 and COX-2 targets. While on the iNOS target,

none of the compounds were selective and had the same geometric 3D structure. This is indicated by the absence of compounds that produce hits and the pharmacophore fit score. The following (fig. 2) is the result of visualizing the structure that produces hits on COX-1 and COX-2 targets in 2D and 3D structures (fig. 2) [20, 21].

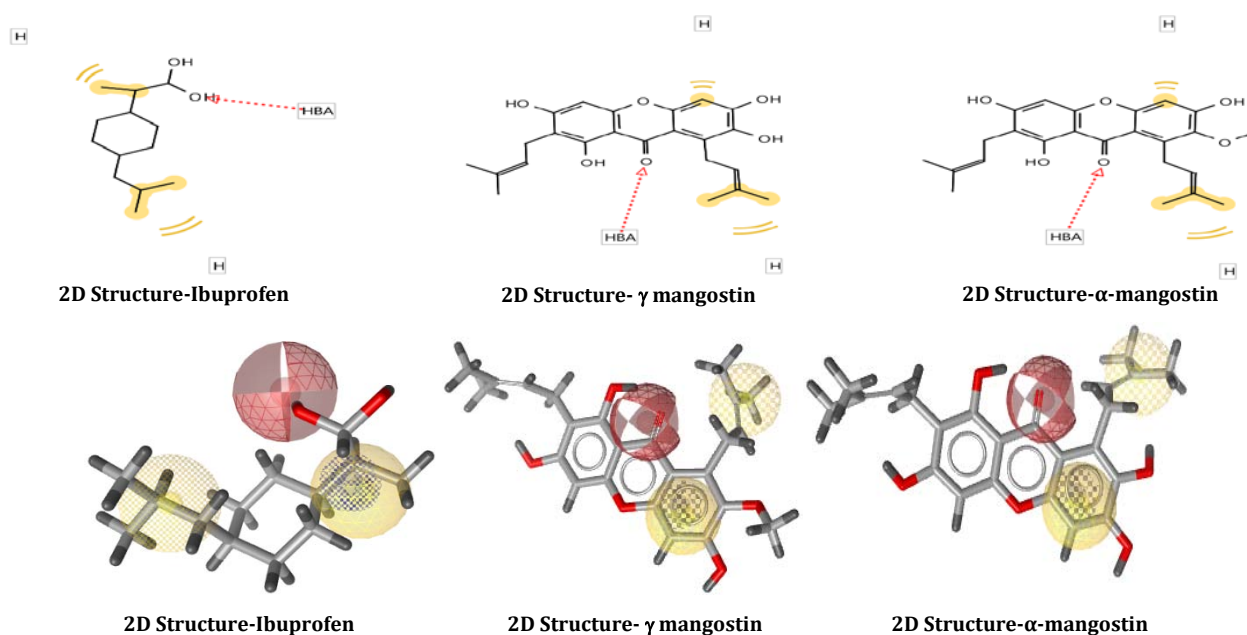


Fig. 2: Visualization for 2D and 3D of COX-1 with compound hits

As shown in fig. 3., Chemical features i.e. positively ionized, hydrophobic interactions, hydrogen bond donors, and acceptors, are represented as blue stars, yellow circled, green arrows, and red arrows, respectively. The interaction between the COX-1 or COX-2 target with the test compound was mainly hydrophobic and hydrogen bonding interactions existed in all compounds that had hits on the COX-1 and COX-2 targets [20, 9].

Enzyme preparation of iNOS, COX-1, and COX-2

The iNOS, COX-1, and COX-2 receptors had several A, B, C, and D chains. The natural ligand inhibitor of iNOS was L-arginine located throughout the iNOS protein chain and the A chain was used in the receptor preparation process of this study. Likewise, with the COX-1 receptor, the natural ligand used was ibuprofen in the entire chain of the enzyme receptor, but the chain used in this study was the A

chain. In addition to the natural COX-2, the ligand used was celecoxib attached to the A chain [22].

The preparation of the iNOS, COX-1 and COX-2 enzyme receptors was carried out by removing the natural ligands for each selected chain so the space can be used for docking the test compound. In addition, the elimination of water molecules (H_2O) on the receptor structure was carried out to hinder the tethering process and only ligands and receptors interacted [23]. The receptors; iNOS, COX-1, COX-2, and the ligands; L-arginine, ibuprofen, and celecoxib were stored in PDB files.

Validation molecular docking

The validation of the molecular docking method was carried out by validating the binding of iNOS, COX-1, and COX-2 receptors with the native ligands using the Autodock Tools 1.5.6 program. Table 1 represents the results and display of the interactions.

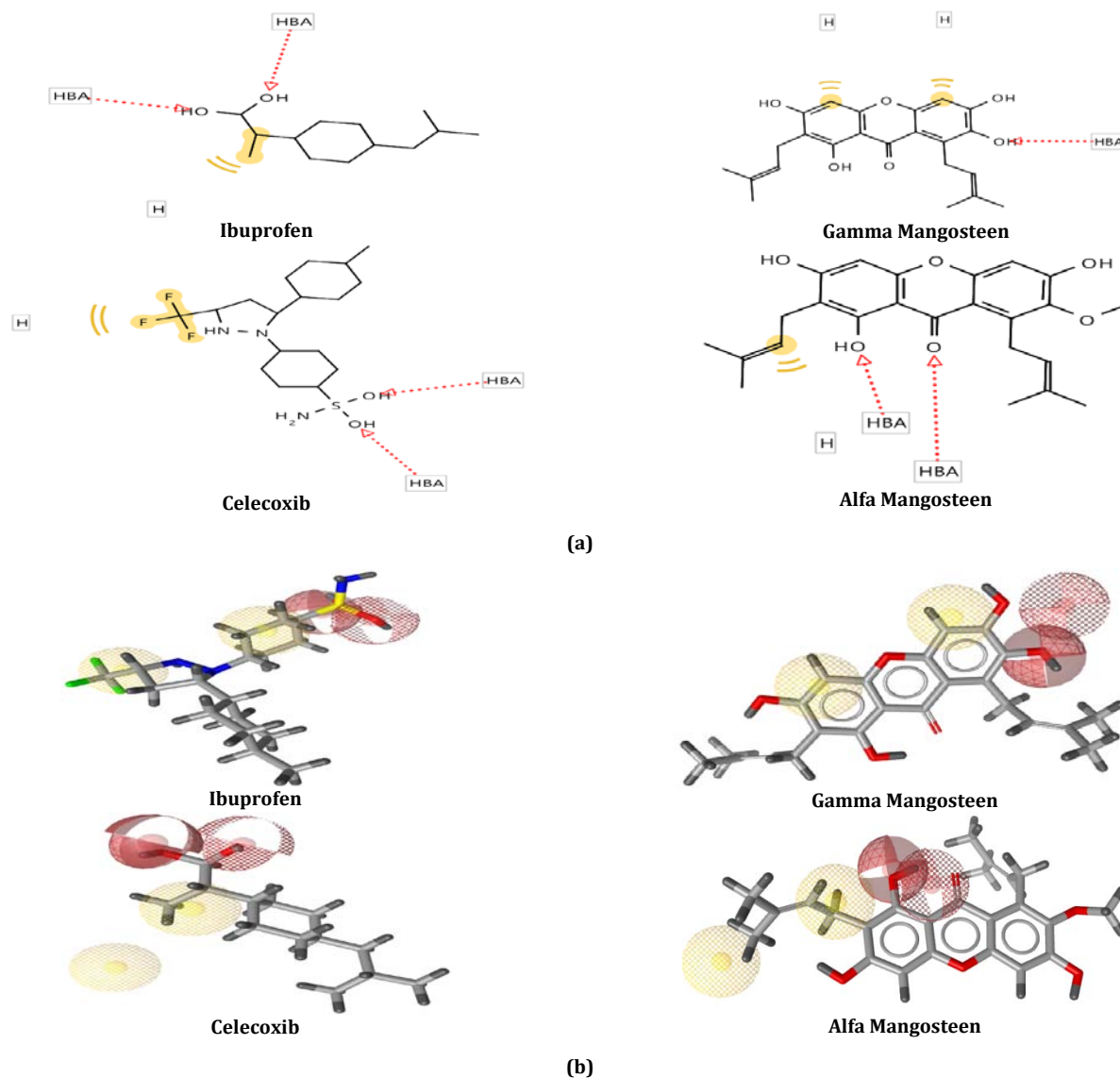


Fig. 3: Visualization for 2D and 3D of COX-2 with compound hits using pharmacophore modeling

Table 2: Results of molecular docking validation

Receptor	Native ligand	ΔG° (Kcal/mol)	Ki	RMSD (Å)	AA Residue	Hydrogen bond
iNOS (PDB: 1NSI)	L-arginine	-4.81	300.45 μ M	1.554	Gln263, Arg266, Arg388, Asp382, Tyr347, Gln377, Tyr373, Pro350,	Glu377, Tyr373, Tyr347, Pro350
COX-1 (PDB: 1EQG)	Ibuprofen	-8.38	716.18 nM	0.887	Leu531, Arg120, Val116, Tyr355, Leu359, Ala527, Ser353, Val349, Ile523, Phe518, Trp387, Tyr385, Met522, Gly526, Phe381, Leu352	Arg120 Tyr355
COX-2 (PDB: 3LN1)	Celecoxib	-10.92	9.84 nM	0.921	His75, Leu338, Val509, Gly512, Phe504, Arg499 Gln178, Ala502, Ile503, Ser339, Leu517, Val335 Leu345 Tyr341, Arg106 Ala513, Leu370 Tyr371, Trp373, Met508	His75 Phe504 Arg499

The validation results of the iNOS, COX-1, and COX-2 enzyme binding pockets (code: 1NSI, 1EQG, and 3LN1) through binding validation of natural ligands as shown in table 2. Molecular docking parameters were selected with 50 runs and grid boxes varied according to the enzyme used. The free binding energy of L-arginine with iNOS is -4.81 kcal/mol, with an inhibition constant of 300.45 nM, and an RMSD of 1.554 at amino acid residues Gln263, Arg266, Arg388, Asp382, Tyr347, Gln377, Tyr373, and Pro350. The hydrogen bonds formed between L-arginine and iNOS enzymes were Glu377, Tyr373, Tyr347, and Pro350.

Furthermore, Ibuprofen and COX-1 enzyme give binding energy of -8.38 kcal/mol, an inhibitory constant of 716.18 nM, and amino acid residue RMSD of 0.887 consisting of Leu531, Arg120, Val116, Tyr355, Leu359, Ala527, Ser353, Val349, Ile523, Phe518, Trp387, Tyr385, Met522, Gly526, Phe381, Leu352. The hydrogen bonds formed were Arg120 and Tyr355, with distances of 2.59 and 2.86 Å.

Interaction of Celecoxib and COX-2 enzyme resulted from free energy binding of -10.92 kcal/mol, inhibition constant of 9.84 nM, and RMSD of 0.921 with amino acid residues of His75, Leu338,

Val509, Gly512, Phe504, Arg499, Gln178, Ala502, Ile503, Ser339, Leu517, Val335, Leu345, Tyr341, Arg106, Ala513, Leu370, Tyr371, Trp373, and Met508. The hydrogen bonds formed between the natural ligand and the COX-2 enzyme were His75 with a distance of

2.13 Å. Phe504 with a distance of 3.15, and Arg499 with a distance of 3.27 Å. Each RMSD (Root mean square deviation) is <math> < 2 \text{ \AA}</math>, hence the results are considered valid. The visualization results of docking validation of iNOS, COX-1, and COX-2 are shown in fig. 4.

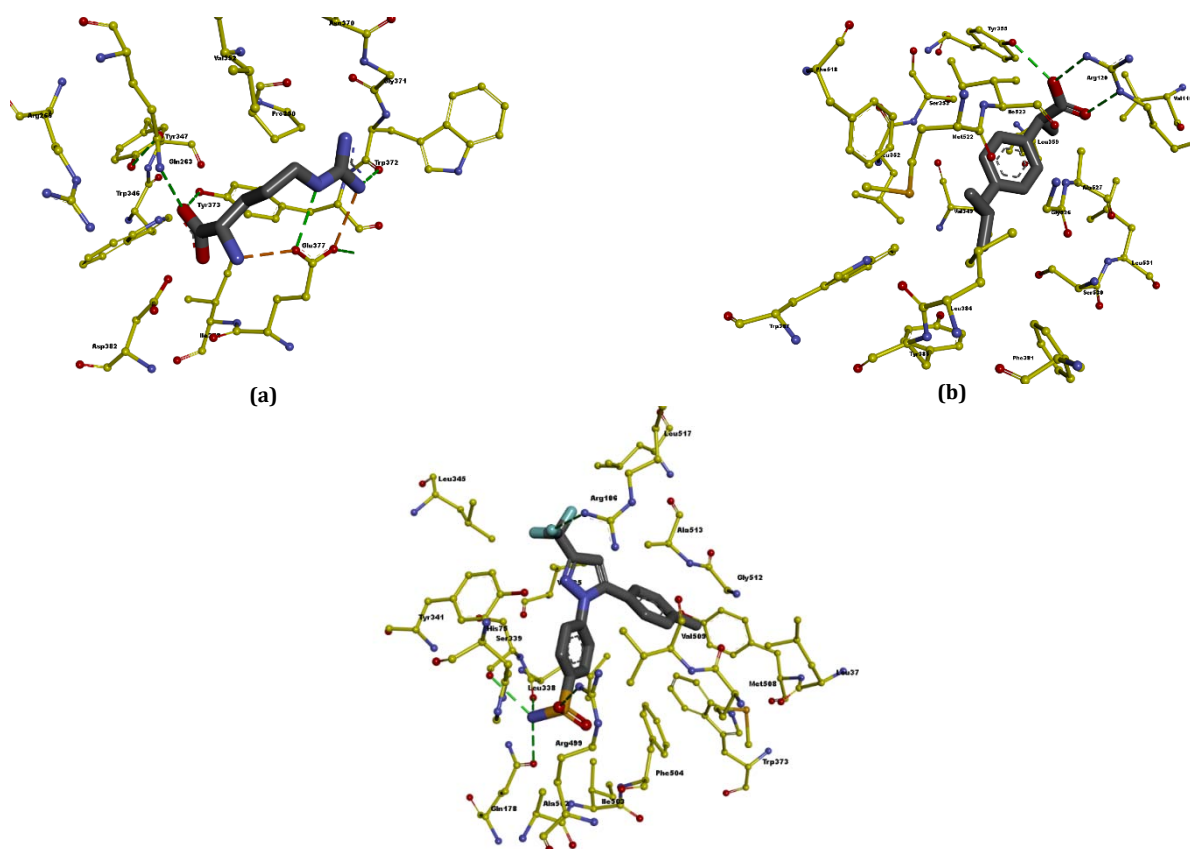


Fig. 4: Molecular docking visualization of (a) iNOS and L-arginine, (b) COX-1 and ibuprofen, and (c) COX-2 and celecoxib

The docking results for each test ligand on iNOS, COX-1, and COX-2 enzymes were fairly uniform between the test compound and the docking validation. The number of conformations produced was

quite significant. The bonds were almost similar to the results of the validation process. Table 3 represents the binding results of the three enzymes to the test compounds α -mangosteen.

Table 3: Molecular docking results of the test compound α -mangosteen

Receptors	ΔG° (Kcal/mol)	Ki	RMSD (Å)	AA residue	Hydrogen bond
iNOS	-5.09	186.77 μM	64.963	Ile201, Cys200, Pro350, Glu377, Gln263, Tyr347, Tyr373, Asp382, Arg381, Arg266	Arg266 Asp382 Tyr373 Tyr374
COX-1	-5.00	215.84 μM	204.504	Ser530, Tyr385, Phe381, Trp387, Gly528, Leu384, Phe518, Met522, Leu352, Ser353, Ile523, Ala527, Val349, Tyr355, Leu531, Arg120, Val116, Leu93, Leu359, Ile345, Met133	Tyr355
COX-2	-6.15	31.01 μM	38.307	Arg499, His75, Ser339, Val509, Tyr341, Ala513, Val102, Leu517, Met99, Ile311, Leu345, Val335, Arg105, Ser516, Tyr371, Gly512, Trp373, Met508, Phe508, Gln178, Leu338, Ile503, Ala502	Tyr341

Molecular docking of the iNOS enzyme with the test compound showed that α -mangosteen interacted with the active site of the iNOS enzyme through hydrogen bonds. A hydrogen bond is formed by a hydroxy group in the center of the structure, an amide group (peptide bond), and/or other groups that can become hydrogen bond donors or acceptors. In drug design, hydrogen bonding is exploited to obtain specificity, which was achieved t only through favorable specific short-range directional interactions, but also through ligand-receptor arrangement leaving the binding capacity less favorable. The number of hydrogen bonds in the drug molecule might be limited by the requirements on polarity by absorption and permeation [15].

Lipinski's rule of five stated that compounds with more than 5 hydrogen bond donors or more than 10 hydrogen bond acceptors are more likely to have poor absorption or permeation characteristics

[13]. Hydrogen bonds formed between α -mangosteen and iNOS enzymes at residues Arg266 Asp382 Tyr373, and Tyr374 with a bond distance of 3.25, 2.10, 3.29, and 3.35 Å that bound to O and OH atoms in the third chain of the α -mangosteen structure. The resulting binding energy was 5.09 Kcal/mol. The α -mangosteen compound has a fairly large bond-free energy of 5.00 Kcal/mol and Inhibitory constants of 215.84 nM. The α -mangosteen compound formed hydrogen bonds with the amino acid residue Tyr355 with a distance of 2.63 Å. The results showed that it was a significant value with small binding energy and good clusters. The α -mangosteen formed hydrogen bonds with residues of Tyr341 with a distance of 2.46. For the hydrophobic bonds, α -mangosteen bound to residues Phe504, Leu517 Val335, Leu 345, and Ile331 via the alkyl and methoxy groups on the side chain of α -mangosteen. This is related to Dermawan *et al.* (2018), who stated that hydrophobic bonds in drug-receptor interactions are very

important because they greatly affect the absorption and permeation process of a drug or a compound [24].

The hydrogen and hydrophobic bonds resulting from the binding of the α -mangosteen to the COX-2 receptor amino acid residues,

including Arg499, His75, Ser339, Val509, Tyr341, Ala513, Val102, Leu517, Met99, Ile311, Leu345, Val335, Arg105, Ser516, Tyr371, Gly512, Trp373, Met508, Phe508, Gln178, Leu338, Ile503, and Ala502. The resulting binding energy was 6.15 Kcal/mol and the inhibitory constant (K_i) was 31.01 μ M.

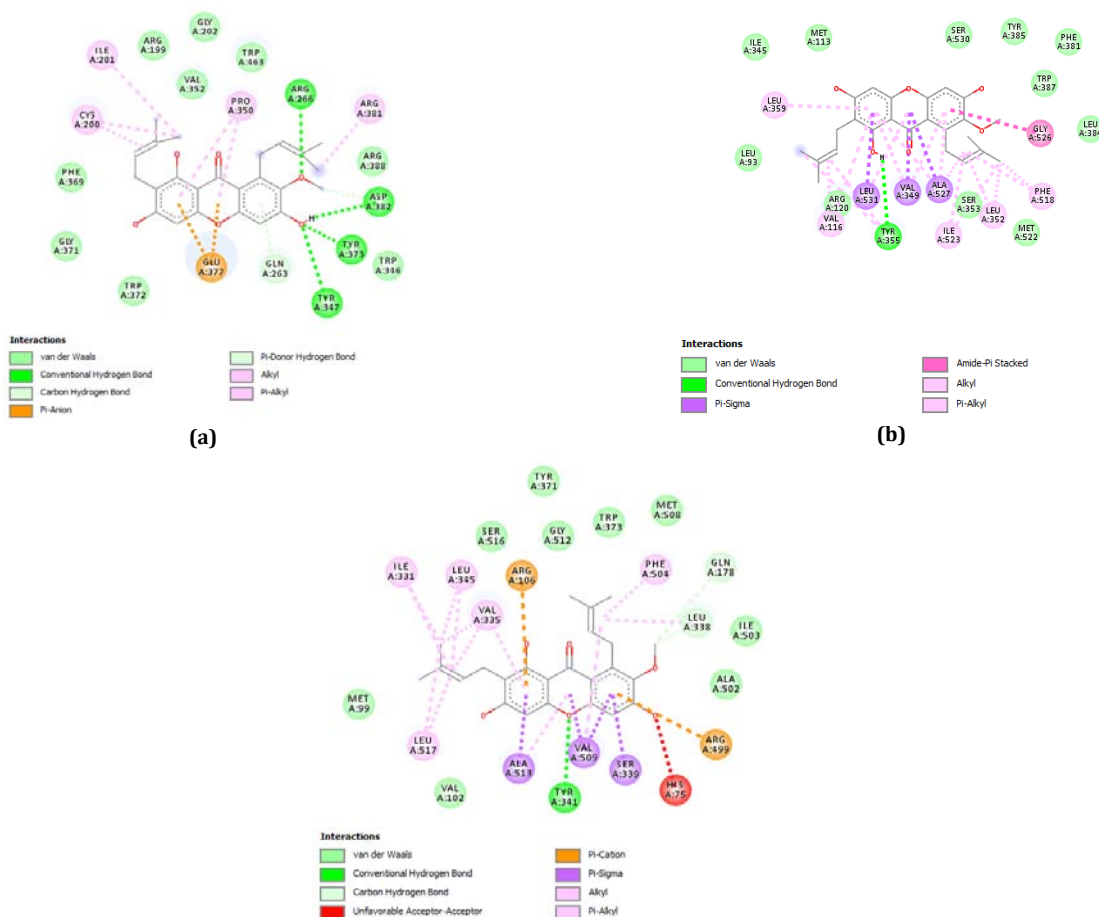


Fig. 5: Interactions of α -mangosteen against (a) iNOS, (b) COX-1, and (c) COX-2

The molecular docking results of α -mangosteen to iNOS, COX-1, and COX-2 receptors were directly proportional to previous studies, such as Mohan (2018) [25]. The research reported that two xanthenes compounds, namely α -mangosteen and γ -mangosteen isolated from the pericarp of *G. mangostana* significantly inhibited the production of nitric oxide and PGE2 from RAW cells 246,7 and stimulated lipopolysaccharide (LPS) [15]. The visualization of the molecular docking of the test compound of α -mangosteen can be seen in fig. 5.

Molecular docking of γ -mangosteen on the iNOS, COX-1, and COX-2 enzymes gave fairly uniform results between the binding process of the test compound and the results of the previous re-docking validation. The number of conformations produced was quite significant. The bonds produced were almost the same as the bonds from the validation results. The docking results of the three enzymes to the test compounds α -mangosteen and γ -mangosteen can be seen in the following table 3.

Table 4: Molecular docking results of γ -mangosteen against iNOS, COX-1, and COX-2

Receptors	AG °(Kcal/mol)	Ki μ M	RMSD (Å)	AA Residue	Hydrogen bond
iNOS	-6.76	11.14 μ M	65.084	Trp463, Gly202, Cys200, Phe369, Val352, Gly371, Ala351, Pro350, Asn370, Glu377, Gln263, Tyr373, Tyr347, Trp346, Asp382, Arg388, Arg381	Asp382, Tyr347, Tyr373, Pro350
COX-1	-5.30	130.52 μ M	204.145	Phe518, Gly526, Leu384, Met522, Ile523, Leu352, Ala527, Val349, Tyr355, Arg120, Leu93, Leu531, Ile345, Val116, Leu117, Met113, Leu359, Tyr348, Trp387, Phe381, Ser530, Tyr385	Arg120, Met522
COX-2	-7.81	1.90 μ M	37.554	His75, Ile178, Gln178, Tyr341, Ser339, Leu338, Val335, Leu517, Pro514, Ala513, Ser516, Gly512, Met508, Phe504, Tyr371, Trp373, Leu370, Phe367, Val509, Ala502, Gly505, Arg499	His75, Ser339, Ala513

As shown in table 4, The binding of the γ -mangosteen molecule to the iNOS enzyme showed good results with a free bond energy of -6.76 kcal/mol and inhibitory constant of 11.14 μ M with amino acid residues of Phe593, Gly594, Tyr631, Phe634, Arg633, Cys635,

Gly596, Gly627, Thr592, Ser591, Ser628, Glu546, Thr545, Ser550, Leu626, Lys549, Gln665, Glu661, and Thr547. The hydrogen bonds formed between residues Asp382, Tyr347, Tyr373, and Pro350 to the hydroxyl group on the γ -mangosteen compound. The residue

distances with the binding receptor were 1.84, 3.40, 2.90, and 2.23 Å, respectively. The results of the tethering of this molecule were promising.

Meanwhile, molecular docking of γ -mangosteen to COX-1 resulted in a binding energy value of -5.30 Kcal/mol, an inhibition constant of 130.52 M and the residues produced in this tethering includes Phe518, Gly526, Leu384, Met522, Ile523, Leu352, Ala527, Val349, Tyr355, Arg120, Leu93, Leu531, Ile345, Val116, Leu117, Met113, Leu359, Tyr348, Trp387, Phe381, Ser530, and Tyr385. The hydrogen bonds formed at residues of Arg120 with a distance between the receptor and the ligand at 1.62 Å and Met522 at a distance of 2.25 Å that bound to the receptor at the hydroxyl group OH. In addition, the binding of COX-1 to γ -mangosteen formed a hydrogen bond by residues Tyr355 and Ser353 with a distance of 3.58 and 3.26 Å. The residues and bonds formed with the γ -mangosteen were almost the same as the bond in the validation process. The value of bond-free energy required for γ -mangosteen was significant, although higher than the docking energy produced during the process validation.

Finally, the binding results of γ -mangosteen to the COX-2 yielded the best results as compared to the binding between iNOS and COX-1 to α -mangosteen and γ -mangosteen. The results of the tethering showed that the required free energy was 7.81 Kcal/mol and the inhibition constant (K_i) was 1.90 μ M. The residues and bonds formed at γ -mangosteen were the same as the residues formed at the beginning, which were The178, Gln178, Tyr341, Ser39, Leu338, Val335, Leu517, Pro514, Ala513, Ser516, Gly512, Met508, Phe504, Tyr371, Trp373, Leu370, Phe367, Val509, Ala502, Gly505, and Arg499. The hydrogen bonds formed by His75 had a bond distance of 2.48 Å, the residue, Ser339, with a bond distance of 1.75 Å, and Ala513 with a bond distance of 2.31 Å. This hydrogen bond is bound to the hydroxyl group by bonding to the O-H in the C chain. 3, 6, and 7.

The hydrogen bond formed on the binding of COX-2 to γ -mangosteen was almost the same as the hydrogen bond in celecoxib, where the hydrogen bond formed was at His75. This result showed that γ -mangosteen could also bind to important amino acid residues, His75 in the COX-2 binding pocket, similar to binding with celecoxib. The visualization of the molecular docking of γ -mangosteen can be seen in fig. 6.

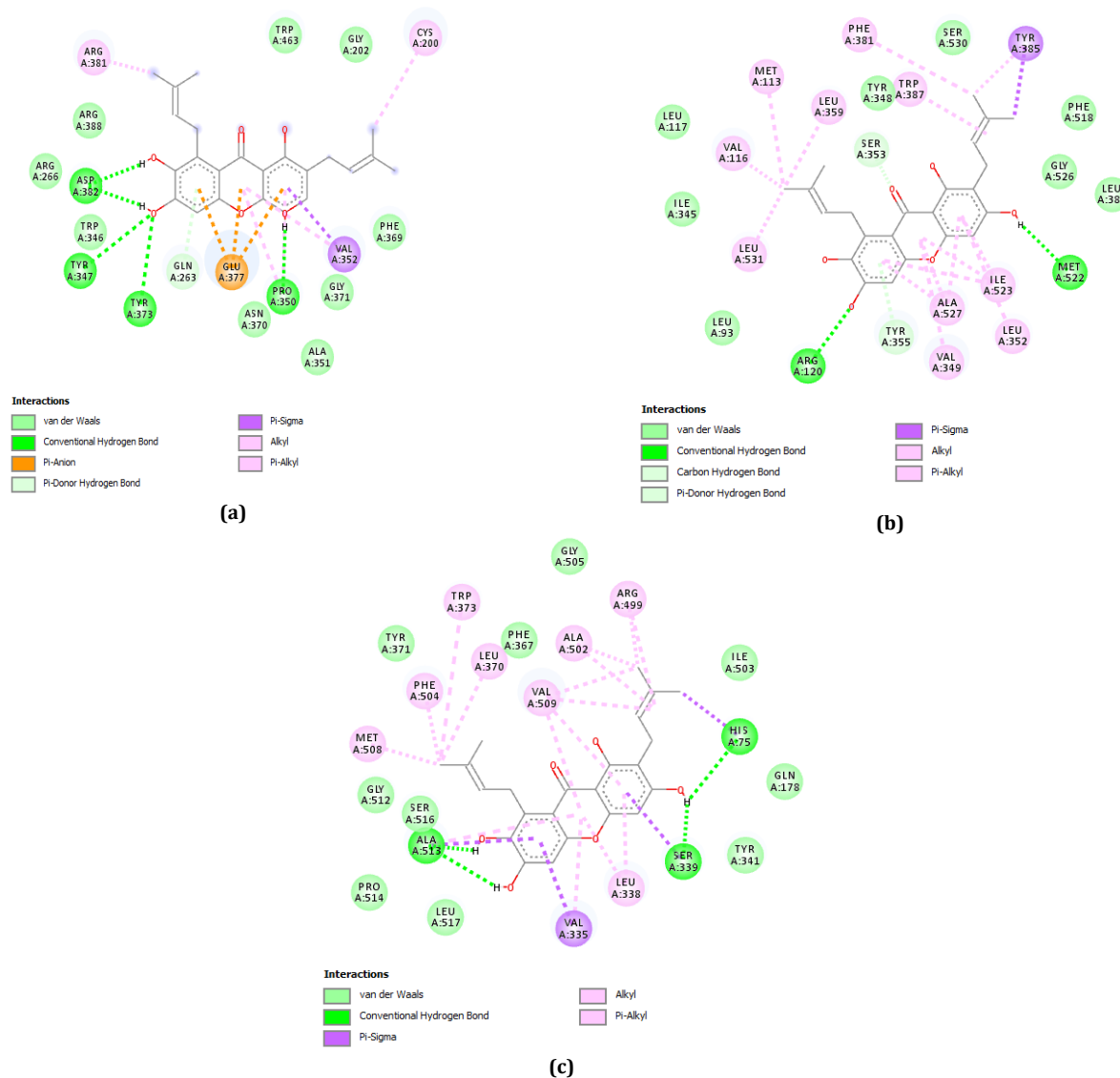


Fig. 6: Interactions of γ -mangosteen against (a) iNOS, (b) COX-1, and (c) COX-2

The results of the superimpose α -mangosteen and γ -mangosteen (fig. 7) showed better results for the COX-2 binding receptor than the iNOS and COX-1 receptors. This is similar to the research

reported by [26], where COX-2, was a selective target for good anti-inflammatory drugs. COX-1 inhibition has side effects associated with anti-inflammatory COX inhibitors. Therefore, γ -mangosteen

was a test compound that produced a low value of bond-free energy, hence the best compound as an anti-inflammatory agent compared to the α -mangosteen compound. In its characteristics, the test compounds of α -mangosteen and γ -mangosteen had several different and unique characteristics, that could be one of the factors causing γ -mangosteen to produce a fairly good molecular docking value as in the research [27].

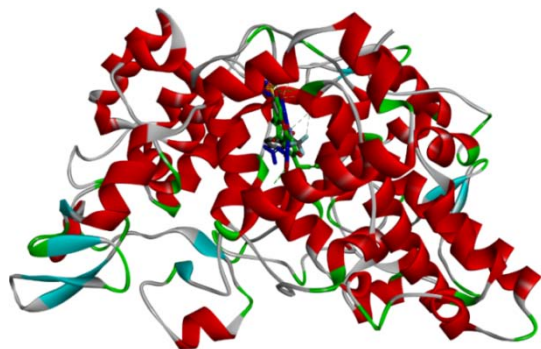


Fig. 7: Superimpose γ -mangosteen (green carbon), and α -mangosteen (blue carbon) with celecoxib (grey carbon) in the binding site of COX-2

CONCLUSION

In the virtual pharmacophore screen, γ -mangosteen and α -mangosteen were selective against COX-1 and COX-2 but t-selective for iNOS targets. The highest pharmacophore fit score on COX-1 and COX-2 was γ -mangosteen. The interaction of α -mangosteen and γ -mangosteen compounds to the binding site of iNOS, COX-1, and COX-2 forms hydrogen bonds, hydrophobic bonds, and hydrogen bonds van der Waals. The best binding iNOS between the γ -mangosteen test compound and the COX-2 enzyme receptor. The binding energy values generated from molecular docking of each test compound; α -mangosteen and γ -mangosteen to iNOS, COX-1, and COX-2 receptors were -5.09 Kcal/mol, -5.00 Kcal/mol, and -6.15 binding energy and -6.76 Kcal/mol, -5.30 Kcal/mol and -7.81 Kcal/mol respectively. α -mangosteen and γ -mangosteen show good molecular interaction with iNOS, COX-1, and COX-2 receptors hence contributing to the anti-inflammatory activity.

ABBREVIATIONS

COX-1: Cyclooxygenase-1, COX-2: Cyclooxygenase-2, iNOS: inhibitor Nitric Oxide synthase, HIV: Human Immunodeficiency Virus, PG: Prostaglandins, AA: Arachidonic Acid, PGE: Prostaglandin E2, TNF: Tumor Necrosis Factor, LPS: Lipopolysaccharide, AUC: Area Under Curve, EF: Enrichment Factor, PDB: Protein Data Bank, ROC: Receiver Operating Characteristics, RMSD: Root Mean Standard Deviation

ACKNOWLEDGEMENT

The authors thank the Ministry of Education and Culture of Republic of Indonesia for financially support the research through Applied research (2064/UN6.3.1/PT.00/2022).

FUNDING

Nil

AUTHORS CONTRIBUTIONS

All the authors have contributed equally.

CONFLICT OF INTERESTS

The authors declare that we have conflicts of interest in this work.

REFERENCES

1. Muchtaridi M, Suryani D, Qosim WA, Saptarini NM. Quantitative analysis of A-mangostin in mangosteen (*Garcinia mangostana*

L.) pericarp extract from four district of west Java by HPLC method. *Int J Pharm Pharm Sci.* 2016;8:232-6.

- Marzaimi IN, Aizat WM. Current review on mangosteen usages in antiinflammation and other related disorders. 2nd ed. Elsevier Inc; 2019.
- Muchtaridi M, Wijaya CA. Anticancer potential of α -mangostin. *Asian J Pharm Clin Res.* 2017;10(12):440-5. doi: 10.22159/ajpcr.2017.v10i12.20812.
- Yatman E. Mangosteen rind contains high nutritious xanthenes. *Univ Borobudur.* 2012;29:2-9.
- Putri IP. Effectivity of xanthone of mangosteen (*Garcinia mangostana* L.) rind as anticancer. *J Major.* 2015;4:33.
- Dinata DI, Suryatno H, Musfiroh I, Suherman SE. Molecular docking simulation of xanthorrhizol compounds derived from temulawak as antiinflammatory on enzymes COX-1 and COX-2. *IJPST.* 2014;1(1):7-13. doi: 10.15416/ijpst.v1i1.7508.
- Liu SH, Lee LT, Hu NY, Huange KK, Shih YC, Munekazu I. Effects of alpha-mangostin on the expression of anti-inflammatory genes in U937 cells. *Chin Med.* 2012;7(1):19. doi: 10.1186/1749-8546-7-19. PMID 22920833.
- Sukma M, Tohda M, Suksamran S, Tantisira B. γ -mangostin increases serotonin 2A/2C, muscarinic, histamine and bradykinin receptor mRNA expression. *J Ethnopharmacol.* 2011;135(2):450-4. doi: 10.1016/j.jep.2011.03.039, PMID 21440614.
- Musfiroh I, Megawati G, Herawati DMD, Rusdin A. 3D-pharmacophore modelling of Omega-3 derivatives with peroxisome proliferator-activated receptor gamma as an anti-obesity agent. *Int J App Pharm.* 2021;13Special Issue 4:167-70. doi: 10.22159/ijap.2021.v13s4.43851.
- RCSB Protein Data Bank, Protein Data Bank. org/Pdb; 2020. Available from: <http://www.rcsb.org>. [Last accessed on 30 Mar 2020]
- Pubchem, PubChem; 2020. Available from: <https://pubchem.ncbi.nlm.nih.gov/> [Last accessed on 01 Apr 2020]
- Mysinger MM, Carchia M, Irwin JJ, Shoichet BK. Directory of useful decoys, enhanced (DUD-E): better ligands and decoys for better benchmarking. *J Med Chem.* 2012;55(14):6582-94. doi: 10.1021/jm300687e, PMID 22716043.
- Nurhidayah M, Fadilah F, Arsianti A, Bahtiar A. Identification of Fgfr inhibitor as St2 receptor/interleukin-1 receptor-like 1 inhibitor in chronic obstructive pulmonary disease due to exposure to E-cigarettes by network pharmacology and a molecular docking prediction. *Int J App Pharm.* 2022;14:256-66. doi: 10.22159/ijap.2022v14i2.43784.
- Praceka MS, Megantara S, Mustarichie R. Journal of Global Pharma Technology Molecular Modeling of Anti-Alopecia Compounds Found in Sauropus Androgynus. *Molecular Modeling of Anti-Alopecia Comfounds Found in Sauropus Androgynus;* 2020. doi:10.13140/RG.2.2.25592.67848
- Shaikh SI, Zaheer Z, Mokale SN, Lokwani DK. Development of new pyrazole hybrids as antitubercular agents: synthesis, biological evaluation and molecular docking study. *Int J Pharm Pharm Sci.* 2017;9(10):50. doi: 10.22159/ijpps.2017v9i11.20469.
- Holik HA, Ibrahim FM, Wianatalie E, Achmad A, Faried A, Kartamihardja AHS. The molecular interaction and admet prediction of modified Jph203 as a potential radiopharmaceutical kit for molecular imaging of cancer: an *in silico* research. *Int J App Pharm.* 2021;13Special Issue 4:205-9. doi: 10.22159/ijap.2021.v13s4.43860.
- Wolber G, Langer T. LigandScout: 3-D pharmacophores derived from protein-bound ligands and their use as virtual screening filters. *J Chem Inf Model.* 2005;45(1):160-9. doi: 10.1021/ci049885e, PMID 15667141.
- Hariyanti H, Kurmardi K, Yanuar A, Hayun H. Ligand-based pharmacophore modeling, virtual screening, and molecular docking studies of asymmetrical Hexahydro-2H-Indazole analogs of curcumin (AIACs) to discover novel estrogen receptors alpha (ER α) inhibitor. *Indones J Chem.* 2020;21(1):137. doi: 10.22146/ijc.54745.
- Alamri MA, Alamri MA. Pharmacophore and docking-based sequential virtual screening for the identification of novel

- sigma 1 receptor ligands. *Bioinformation*. 2019;15(8):586-95. doi: 10.6026/97320630015586, PMID 31719769.
20. Temml V, Kaserer T, Kutil Z, Landa P, Vanek T, Schuster D. Pharmacophore modeling for COX-1 and -2 inhibitors with LigandScout in comparison to discovery studio. *Future Med Chem*. 2014;6(17):1869-81. doi: 10.4155/fmc.14.114, PMID 25495981.
 21. Levita J, Patala R, Kolina J, Milanda T, Mutakin M, Puspitasari IM. Pharmacophore modeling and molecular docking of phytoconstituents in *Morus* sp. and *Arcangelisia flava* against nitric oxide synthase for antiinflammatory discovery. *J App Pharm Sci*. 2018;8(12):53-9. doi: 10.7324/JAPS.2018.81207.
 22. Nugraha G, Istyastono EP. Virtual target construction for structure-based screening in the discovery of histamine H2 receptor ligands. *Int J Appl Pharm*. 2021;13:239-41. doi: 10.22159/ijap.2021v13i3.41202.
 23. Candra GNH, Wijaya IMAP. Molecular docking kaempferol as an anti-inflammatory in Atherosclerosis *in silico*. *J Ilm Medicam*. 2021;7:13-8.
 24. Bhowmik R, Roy S, Sengupta S, Sharma S. Biocomputational and pharmacological analysis of phytochemicals from *Zingiber officinale* (Ginger), *allium sativum* (garlic), and *murrayakoenigii* (curry leaf) in contrast to type 2-diabetes. *Int J App Pharm*. 2021;13:280-6. doi: 10.22159/ijap.2021v13i5.42294.
 25. Silalahi M. Benefits and bioactivity of Mangist (*Garcinia mangostana* L.). *Bioeducation*. 2021;12:30-7.
 26. Mohan S, Syam S, Abdelwahab SI, Thangavel N. An anti-inflammatory molecular mechanism of action of α -mangostin, the major xanthone from the pericarp of *Garcinia mangostana*: an *in silico*, *in vitro* and *in vivo* approach. *Food Funct*. 2018;9(7):3860-71. doi: 10.1039/c8fo00439k, PMID 29953154.
 27. Kurniawan. Isolation, identification, validation of determination of Alfa mangostin and gamma mangostin levels of Mangostine fruit (*Garcinia mangostana* L.). *Universidat Muhammadiyah Surakarta*; 2020. p. 4-5.